Renewable energy based catalytic CH$_4$ conversion to fuels

J. Baltrusaitis,[*ab] I. Jansen[c] and J. D. Schuttlefield Christus[*c]

Natural gas is envisioned as a primary source of hydrocarbons in the foreseeable future. With the abundance of shale gas, the main concerns have shifted from the limited hydrocarbon availability to the sustainable methods of CH$_4$ conversion to fuels. This is necessitated by high costs of natural gas transportation in its native gaseous form. Conventional gas-to-liquid conversion technologies are capital and scale intensive and can hardly be envisioned in their current form to be cost efficient in the remote locations of the natural gas extraction sites. Solar energy can be utilized at the gas extraction site to perform catalytic CH$_4$ conversion using electrons obtained *via* photovoltaics or directly with photons. We provide broader insight into the catalytic CH$_4$ conversion methods that utilize renewable energy *via* photo(electro)catalytic processes, with particular focus on the catalytic materials used, reaction conditions and intermediates, as well as their selectivity. Based on the currently available scientific literature, we propose several hybrid catalytic CH$_4$ conversion processes based on both conventional and renewable – photo(electro)chemical – catalysis.

[a] Department of Chemistry and Biomolecular Engineering, Lehigh University, B323 Iacocca Hall, 111 Research Drive, Bethlehem, PA 18015, USA. E-mail: job314@lehigh.edu, j.baltrusaitis@utwente.nl
[b] PhotoCatalytic Synthesis, MESA+ Institute for Nanotechnology, Faculty of Science and Technology, University of Twente, Meander 229, P.O. Box 217, 7500 AE Enschede, The Netherlands
[c] Department of Chemistry, University of Wisconsin Oshkosh, 800 Algoma Boulevard, Oshkosh, WI 54901, USA. E-mail: schuttlj@uwosh.edu

1. Introduction

Natural gas, with its major component CH$_4$, is and will be in the foreseeable future the main source of hydrocarbons for energy and fuels.[1] Total proven natural gas resources alone in 2012 were 6845 TCF (trillion cubic feet).[2] While it is difficult to predict the exact recoverable gas amounts, current estimations

Jonas Baltrusaitis was born in June 24, 1976 in Marijampole, Lithuania. He graduated from Kaunas University of Technology, Lithuania with BSc and MSc degrees in Chemical Engineering in 1998 and 2000 and then worked in the chemical industry as a process engineer. In 2003 he started graduate studies at the University of Iowa with Vicki Grassian where he graduated in 2007 with a PhD in Physical Chemistry. In 2012,

J. Baltrusaitis

JB became an assistant professor in the Photocatalytic Synthesis Group, University of Twente, The Netherlands. He will join the Lehigh University chemical engineering faculty in Summer 2014 to work on shale gas and hydrocarbon catalysis.

Isaac Jansen is a biochemistry student intending to go to Law School and practice patent law. His undergraduate studies at the University of Wisconsin Oshkosh and the University of Notre Dame have focused primarily on the natural sciences and have been supplemented with philosophy and Japanese language courses. He is currently researching photoelectrochemistry in the Schuttlefield Christus lab at the University of Wisconsin Oshkosh.

I. Jansen

lead to the belief that together with shale gas, it could lead to energy independence for many countries for the decades to come if the resulting increase in the CO_2 footprint can be mitigated. For example, U.S. shale gas production has been projected to increase from 5 TCF in 2010 to 13.6 TCF in 2035, with the latter accounting for 49% of total USA dry gas production.[3] China's proven shale gas reserves are estimated to be 885 TCF – nearly 200 times its annual gas consumption.[4] With the emergence of shale gas, a major paradigm shift occurred when crude oil and natural gas stopped mirroring one another in their price trends (in dollars per million Btu)[5] with natural gas becoming significantly cheaper. Finally, methane hydrates, which are difficult to access crystalline formations containing CH_4, are estimated to account for 317 832 TCF in the USA alone, well beyond the current and future demand for natural gas.[6] From the catalysis science and technology point of view, this availability of CH_4 results in renewed interest in CH_4 conversion techniques that can efficiently and sustainably convert these increasing amounts. Furthermore, direct CH_4 catalytic conversion into liquid hydrocarbons (C_{5+}) or liquid oxygenates *on-site* is of major interest due to the remote location of shale gas extraction facilities and relatively high CH_4 transportation costs. The world's existing fuel infrastructure is predominantly based on liquid hydrocarbons and obtaining them from CH_4 is of major importance.
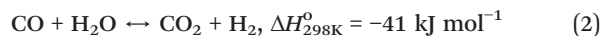
Common catalytic processes to activate CH_4 typically follow one of the two approaches:

Direct endothermic dehydrogenation of CH_4 to $–CH_2$-containing species and H_2 at high temperatures (500–1000 °C). Examples are CH_4 aromatization to yield benzene and H_2 over a Mo-ZSM-5 catalyst and pyrolysis to C_2H_4 and/or C_2H_2 and H_2.[7,8]

Oxidative (and exothermic) dehydrogenation (or partial oxidation) using O_2 or H_2O as a cheap oxidant, as well as other less used oxidants, such as halogens or sulfur. Examples are

partial oxidation of CH_4 to CH_3X (X = OH, Cl, Br or OSO_3H), oxidative coupling to C_2H_6/C_2H_4 and partial oxidation to syngas.[1,9–11]

Oxidatively, CH_4 is converted in refineries into the syngas intermediate to obtain usable H_2 *via* steam reforming (1) on the Ni catalyst followed by water gas shift reaction (2)

$$CH_4 + H_2O \leftrightarrow CO + 3H_2, \Delta H^o_{298K} = 206 \text{ kJ mol}^{-1} \quad (1)$$

$$CO + H_2O \leftrightarrow CO_2 + H_2, \Delta H^o_{298K} = -41 \text{ kJ mol}^{-1} \quad (2)$$

which results in ~8 tons of CO_2 per 1 ton of H_2 generated. On the other hand, typical large scale gas-to-liquid conversion occurring *via* a Fischer–Tropsch or CH_3OH route proceeds *via* slightly exothermic partial oxidation

$$CH_4 + 0.5O_2 \leftrightarrow CO + 2H_2, \Delta H^o_{298K} = -36 \text{ kJ mol}^{-1} \quad (3)$$

followed by Co, Fe or Ru based coupling reactions.[12] These catalytic processes generally apply fairly severe conditions to activate the otherwise stable CH_4 molecule. However, the real challenge here is not the activation step or the severity of conditions required. Instead, it concerns the fact that the desired (intermediate) product is much more reactive than CH_4 and is, therefore, more prone to further oxidation reactions to coke or CO_2 than CH_4 is prone to conversion. Acceptable selectivities are therefore only achieved at a low/moderate conversion level, which results in extensive separation and recycling of unconverted CH_4. The highest yield reported so far decreased with the decreasing thermodynamic stability of the product compared to that of CH_4.[13] Technologies that are presently of industrial significance are based on syngas because syngas is thermodynamically favored over CH_4 under the applied reaction conditions and, therefore, is produced in high yield. This also presents a major challenge in ensuring sustainable CH_4 conversion to liquid fuels, where selective activation of the C–H bond with minimal conversion to CO_2 is critical.[5] Other oxidative approaches that apply oxidants other than O_2, *e.g.* Cl_2, H_2SO_4/SO_3, H_2O_2 and superacids, have also been considered. However, in all of these, an expensive oxidant is eventually regenerated with O_2 resulting in additional processing steps and byproducts.

Relatively inexpensive sources of external energy to activate CH_4 are currently available directly from the sun or utilizing photovoltaic (PV) and wind generated electrons. This is due to the fact that approximately 120 000 TW of solar light strikes the Earth's surface[14] and only a tiny fraction of it is currently utilized, mostly as electricity.[15] With the increasing solar light utilization, unprecedented energy storage challenges have recently been encountered. For example, 200 000 blackouts exceeding three minutes were reported in Germany in 2011 due to the misbalance of the electrical grid resulting from the peak demand for renewable electricity.[16] A way to mitigate this is by storing solar energy in the liquid hydrocarbon form.[17]

Fig. 1 shows the approximate locations of shale gas reserves superimposed on Global Horizontal Irradiation (GHI) maps.[18,19]

Jennifer Schuttlefield Christus earned a B.S. degree in Chemistry and a B.A. degree in Economics from the University of Iowa in 2003. As an undergraduate, she worked at the Center for Advanced Drug Development and later went back to graduate school at the University of Iowa where she received her Ph.D. working under Vicki H. Grassian and Norbert Pienta. She joined Bruce Parkinson's group at the University of Wyoming as a postdoctoral associate in 2008. Currently she is an Assistant Professor at the University of Wisconsin Oshkosh. Her current research interests include semiconductor photoelectrochemistry, solar energy conversion, atmospheric reactions on clay mineral aerosols and chemical education.
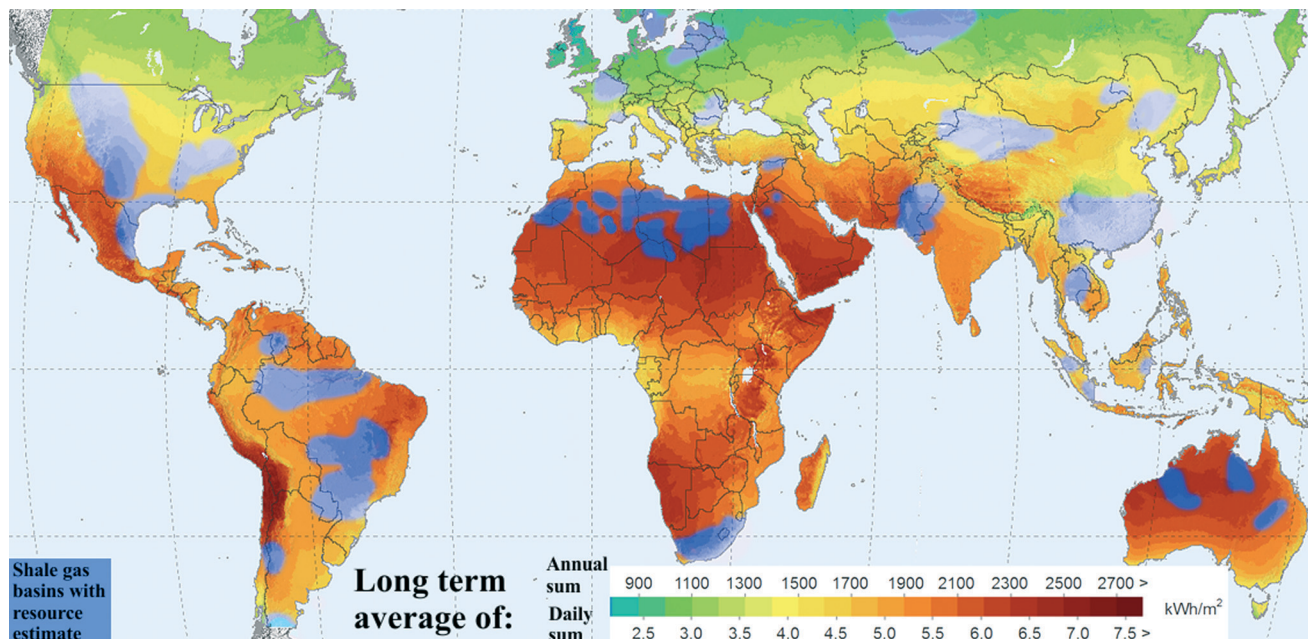
J. D. Schuttlefield Christus

Fig. 1 Locations of the shale gas basins with the available resource estimate in blue, superimposed on the Global Horizontal Irradiation maps (red – highest intensity of incident light and green – lowest).[18,19]

It can be seen that, with the exception of Northern Europe and Russia, the greatest intensity of incident light is available at the shale gas concentration areas, which could thus potentially be utilized for CH_4 conversion. While current developments in utilizing excess electricity mostly focus on the Power2Gas technology of electrocatalytically converting CO_2 to CH_4,[16] we will provide a broader perspective on how electrons can be used instead for CH_4 catalytic conversion. Further, we will provide insights into the possibility of using solar photons directly for CH_4 catalytic conversion, thus bypassing high capital costs incurred in photovoltaic device/electrolyzer manufacturing. Finally, we will try to conceptualize a few CH_4 catalytic conversion processes that would combine both photo(electro)chemical and conventional thermal catalysis to achieve direct CH_4 activation and conversion, facilitated by both electrons and temperature, bypassing reaction intermediates, such as syngas.

2. Renewable energy based CH_4 activation

Electrochemistry and photochemistry can be viewed as emerging opportunities to perform sustainable CH_4 conversion to fuels *on-site* and are, essentially, a variation of the existing conventional catalytic processes. In principle, photo(electro)chemical CH_4 catalytic processes also follow one of the two main routes:

An endothermic route that uses the electrical potential to drive the dehydrogenation reaction

via direct electrochemical oxidation of CH_4 to the unstable radical intermediate $-CH_x- + H_2$ followed by radical coupling to form C_2H_6/C_2H_4 or by addition of a nucleophile (*e.g.* solvent H_2O or a dissolved additive) to form CH_3OH or CH_3Cl.

via indirect oxidation, *e.g.* photoelectrochemical oxidation of the solvent (water) or a dissolved additive (Cl^-) to intermediates that can attack and oxidize CH_4 to a $-CH_x-$ radical, which further reacts with the solvent or additive.

An exothermic oxidation route, *e.g.* using O_2 as the oxidant, which liberates the heat of reaction as electrical potential (*i.e.* fuel cell).

It can be quickly realized that the photo(electro)chemical approach will have to face the same selectivity challenges as the more conventional catalytic routes. These selectivity challenges will therefore have to be considered carefully when analyzing the literature on photo(electro)chemical oxidation of CH_4.

2.1 Electrochemical CH_4 activation

The direct conversion of CH_4 has been a topic of periodic interest. Over the last 50 years, electrochemical studies of CH_4 activation have shown this process to be difficult and energy intensive due to the stability of the CH_4 molecule, the strength of the C–H bond (439 kJ mol^{-1}), low pK_a (pK_a = 48), high ionization potential (12.5 eV) and low proton affinity (4.4 eV).[20–24] Despite ongoing research over several decades, the electrochemical conversion of CH_4 lags in popularity behind obtaining renewable energy *via* water electrolysis and electrochemical carbon dioxide activation.[25] The electrochemical conversion of CH_4 has been extensively reported in the literature for both the electrocatalytic oxidation of CH_4 at metallic anodes and the conversion of CH_4 in fuel cells.[26] E. J. Cairns was the first to review the electrochemical conversion of CH_4 in the early 1970s[27] with more recent reviews focusing on high temperature processes.[28–31] The undeniable advantage of electrochemical processes, however, is their ability to drive catalytic

reactions at room or low (<100 °C) temperatures and pressures and will be the main focus below. The biggest problem here is driving the catalytic process efficiently at room temperatures and pressures[32–34] with inexpensive catalyst materials since most of the research has instead been limited to high temperature fuel cells (Solid Oxide Fuel Cells (SOFC) and Molten Carbonate Fuel Cells (MCFC)).[29,35–37] Though the electrochemical oxidation of CH_4 is thermodynamically favored, the process is kinetically slow.[23] An applied potential to a catalyst surface could potentially reduce the activation energy barrier, influence the nature of the charge-transfer reactions, and potentially stabilize the reaction intermediates on the catalyst surface, influencing which products are produced.[26] Finally, the electrochemical system could be paired with inexpensive sources of external renewable electricity, such as solar (PV technology) and wind, as well as the unbalanced, excess electricity generated at night thus eliminating the need to burn fossil fuels for this conversion process.

2.1.1 High temperature electrochemical CH_4 activation processes. High temperature processes do provide some insight into the electrochemical conversion of CH_4, as an increase in temperature often results in increased reaction rates which tend to be high enough to be practical for use.[30] In addition to the energy needed to use moderate to high temperatures (100–1000 °C), solid state electrolytes that consist of expensive metals or metal oxides doped with rare, expensive elements (ex. palladium, platinum, *etc.*) are most frequently used to electrochemically convert CH_4 because they are effective at withstanding the high temperatures and also efficient at the conversion process.[28,30] Other high temperature methods, such as SOFCs and electrochemical oxygen pumps (EOP), which generally use rare earth oxides and high temperatures, will not be discussed in detail here due to many current reviews.[28,30,38–40] Other moderate temperature processes such as MCFCs, where the complete conversion of CH_4 can be accomplished using appropriate catalysts (*e.g.* Ni-based catalysts),[28,30] have problems with corrosion that tends to reduce cell performance and life. Intuitively, well established conventional catalytic processes, operating nearly at the same temperatures as fuel cells, will outperform the latter in stability and reliability.

2.1.2 Low temperature electrochemical CH_4 activation processes. Low temperature processes (below 100 °C) will be the focus for the remainder of this section. Studies performed at low temperatures are ideal to reduce the amount of energy needed as an input in the conversion process, thus becoming a feasible renewable process. Low temperatures could easily be attained *via* heating with solar concentrators, with the necessary applied potentials generated using PV technology or wind turbines. Electrochemical cells were initially tested for CH_4 activation at low temperatures and room pressure since they have the ability to modify the rates of charge transfer reactions by tuning the cell potential.[30] In early studies of this process as well as in this report, it was recognized that the materials used as electrodes play a key role in the conversion process. The materials can either reduce the activation energy needed to allow the reaction to proceed or they could

stabilize possible useful intermediates. The activation energy of CH_4 can be related to the presence of charged species, which can initiate further CH_4 activation therefore resulting in more ionically charged species.[41,42] Thus the electrochemically controlled cell was developed with the idea that the formation of these species could be controlled and converted into useable products. A summary of experiments performed for the electrochemical oxidation of CH_4 at low temperatures is shown in Table 1. The reaction conditions, the products produced, and the temperature range in which the experiments were run are shown. The intermediates or adsorbed species are also provided and indicated in Table 1 using parentheses. Notably, the majority of these experiments were performed using aqueous electrolytic cells. As can be seen from Table 1, most of the electrodes used are rare metals, such as Pt or Pd, which eventually produce CO_2 when CH_4 is oxidized and generally require a specific electrolyte, such as a strong acid or base. Platinum is widely used due to its high electrocatalytic activity; however, this comes at an expensive price of a limited resource and is unattractive to use on a wide distribution basis.

Furthermore, the data in Table 1 for electrochemical CH_4 activation point to CO_2 and H_2O as the major species produced by the electrochemical activation, with a few exceptions, rather than useful liquid hydrocarbons, though the quantities depend on the conditions at which the activation is performed. This has been theorized to be due to weak and slow chemisorption of CH_4 on the metal electrode surfaces becoming the rate-limiting step[26] and indiscriminate solution generated radical induced bond breaking. Additionally, since the electrochemical activation at low temperatures generally produced complete conversion to CO_2 no selectivities or conversion rates were provided.

Surface studies using molecular beam experiments showed that the sticking coefficient of CH_4 is very low and is little influenced by temperature.[64,65] Recent theoretical studies have shown that CH_4 dissociates on the metal surface to form CH_3, CH_2, and CH[66–68] with –CH– being the most abundant species present when exposed to Pt(100)[68] and Pt(111) surfaces.[67] Chen and Vlachos arrived at a similar mechanism on Pt(111) and Pt(211) surfaces and found that coordination sites, such as steps, are crucial in lowering barriers for dehydrogenation and oxidation.[69] Other metals, such as Co, Rh, Ru, Pd, Ir or Ni, have also been studied theoretically, though to the authors' knowledge these have not been experimentally investigated at lower temperatures.[66,67,70–101] These results have provided some insight into the possible mechanism for activation of CH_4 on different metal surfaces. For example the dissociation of CH_4 on Ni has been shown to occur *via* hollow or bridge sites where Pt appears on the top or edge sites.[66,68] Zhang and co-workers showed in a systematic study of the Pt surfaces (*i.e.* Pt(111), Pt(110) & Pt(100)) that the catalyst can resist carbon deposition providing insight into why Pt has shown high activity for CH_4 activation.[68] In terms of the theoretical examination of the electrooxidation of CH_4, Psofogiannakis and co-workers showed that the dehydrogenation reactions of CH_4 were followed by the oxygenation reactions of the adsorbed CH_x species. This study also suggested that

2400 | Catal. Sci. Technol., 2014, 4, 2397–2411

This journal is © The Royal Society of Chemistry 2014

Table 1 Results of electrochemical activation of CH_4 studies at low temperatures (<100 °C)[26,30]

Temperature (°C)	Electrolyte	Electrode	Products	Experimental details	Method	References
0	From "acidic media to basic media" (SbF_5 to KF), specifically HF +SbF_5	Pt	(CH_3^+), (CH_5^+), ($CH_3^·$), C_2H_6		Linear sweep voltammetry	43
23	2 M $NaClO_4$ in γ-butyrolactone	Pt/C, Co_3O_4, CO_3O_4/C Pt-black	CO_2	0.600–0.800 V $vs.$ Ag/AgCl	Potentiostatic	44
25	0.5–10 M FSO_3H in CF_3COOH & CH_2Cl_2	Pt	($CH_4 \cdots H$)$^+$ → product		CV, electrolysis	45
~25	CH_3CN	Pt microdisk	CH_3^+ + CH_3CN → $CH_3N^+CCH_3$	0.0–4.5 V $vs.$ Ag/AgCl	Linear sweep voltammetry	46
25	0.6 M KCl, pH = 11	Pt	CH_3OH, CH_xCl_{4-x}	1.1–2.0 V $vs.$ SHE 1.3 V $vs.$ SHE	Potentiostatic, photochemical	47–49
25	1 M H_2SO_4; 1 M H_2SO_4 & 0.005 M $FeSO_4$	Cobalt phthalocyanine on carbon (CoPc/C)	CH_2O, HCOOH, CH_3OH, EtOH, CH_3COH	20–30 mA cm^{-2} current density at −0.86 V $vs.$ SHE	$In\ situ$ electrochemical generation, electrolysis, gas chromatography	50
25	0.1–2 M KOH, 2 M NaOH, 0.1 M $NaClO_4$ pH = 11.8	Cu, glassy C, Hg, Au	CH_2O, CH_3OH, CO, CO_2	0.8 to 0.4 V $vs.$ DHE	Potentiostatic	32
25	0.5 M $HClO_4$	Pt, Au, Pd, Ru, Rh	(CO)$_{ads}$, (CHO)$_{ads}$, (COOH)$_{ads}$ → CO_2	0 V to 1.5 V $vs.$ RHE	$In\ situ$ IR spectroscopy, CV	33
~25	0.1 M H_2SO_4 0.5 M $HClO_4$	Pd	(CO) → H_2, CO_2	0.0–1.5 V $vs.$ SHE	Cyclic voltammetry	20
25	(NTf_2)-based ILs	Pt, C, Au	CO_2, H_2O	1.5 to −1.8 V $vs.$ Pt	CV, $in\ situ$ IR spectroelectrochemistry	23
25–65	2.5 M H_2SO_4, 6 M KOH, 3 M $KHCO_3$	Pt-black	CO_2	N/A	Galvanostatic, voltammetry, vapor-phase gas chromatography	51
26	0.5 M H_2SO_4	Pt/Pt	(COH)$_{ads}$, (CO)$_{ads}$		Galvanostatic	52
40–100	1.5 M H_2SO_4–6.5 M KOH	Pt-RANEY®	(CH_x)$_{ads}$ → CO_2		Galvanostatic, potentiostatic	54
60–120	75% H_3PO_4	Pt-black	CO_2		Multipulse potentiodynamic, potentiometric	55
60–120	Nafion-H catalyst	H_2O_2	($H_3O_2^+$) → CH_3OH		Catalytic membrane reactor (3PCMR)	56
65	4.3 M $HClO_4$	Teflon-bonded, Pt-black	C_1 oxygenated hydrocarbon species → CO_2	0.2–1.9 V $vs.$ RHE	Potentiodynamic electrochemical methods	57
80	22 M KF	Pt/Pt	(HCO)$_{ad}$		Potentiostatic, CV	58
80	0.5 M H_2SO_4	Pt/Pt	(CH_3)$_{ads}$ → intermediates → CO_2	−0.110 to 0.100 V $vs.$ SHE	Potentiostatic	59
60, 80–100	0.5 M H_2SO_4	Platinized-Pt	(COH or COOH)$_{ads}$ & (CO)$_{ads}$ → CO_2	0.200–0.800 V $vs.$ RHE	Multipulse potentiodynamic	60, 61
80–90	0.33 M H_3PO_4–0.5 M H_2SO_4	Pt	(CH_x)$_{ads}$ → CO_2		Potentiostatic, coulometry	62
90–110	1.5 M H_2SO_4–8.7 M H_3PO_4	Pt-RANEY®/Au	CO_2	0.270–0.290 V	CV, potentiostatic, galvanostatic	53
5–130	$CF_3SO_3H \cdot H_2O$	Pt	CO_2	0.270–0.290 V	Potentiostatic	63

the CH_4 chemisorption step is the rate-limiting step in the oxidation of CH_4.[67]

Bagotzky $et\ al.$ proposed a generalized chain of the possible steps that are involved in the electrooxidation of CH_4 and other C_1 organics.[102] This network is shown in Fig. 2 for CH_4. Other potential pathways to molecules such as methanol and formic acid have been removed due to experimental observations (shown in Table 1) of complete conversion of CH_4 to carbon dioxide on Pt surfaces.[67]

While Pt has been widely used to study CH_4 electrochemical activation in the past, experimentally the partial electrooxidation methods were originally proposed by Frese using gold, glassy carbon, copper and mercury electrodes that were exposed to CH_4 at room temperature.[32] The electrodes were chosen for various reasons, which include their oxygen reduction capabilities to form peroxides, O_2H^- and O_2^-, at low overpotentials (carbon, Hg, and Au) and effectiveness at oxidizing CH_4 via O_2 at the solid/gas interface (Cu).[32] The electrolytes varied from

$$CH_4 \rightarrow {}^*CH_3 \rightarrow {}^*CH_2 \rightarrow {}^*CH \rightarrow {}^*C$$
$$\downarrow +OH \quad \downarrow +OH \quad \downarrow +OH$$
$${}^*CH_2OH \rightarrow {}^*CHOH \rightarrow {}^*COH$$
$$\downarrow -H \quad \downarrow -H$$
$${}^*CHO \rightarrow {}^*CO$$
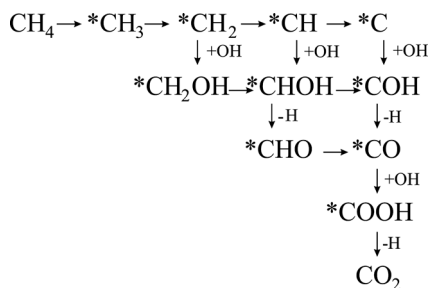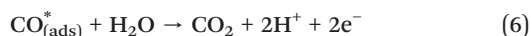$$\downarrow +OH$$
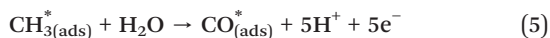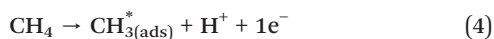$${}^*COOH$$
$$\downarrow -H$$
$$CO_2$$

Fig. 2 The Bagotzky mechanism for the electrooxidation of CH_4.[67,102]

0.01 to 2 M KOH, 0.1 M NaClO$_4$ and 2 M NaOH, with the electrode potentials ranging from +0.8 to +0.4 V *vs.* the dynamic hydrogen electrode (DHE). The products observed by thermal conductivity gas chromatography included CH_2O, CH_3OH, CO and CO_2 where, despite the varied conditions (*e.g.* electrode, electrolyte, stirring rate, *etc.*), the dominant product formed was CH_2O; CO and CO_2 were observed in minor quantities. A relevant finding from this study was the rates of the low temperature processes (10^{-5} to 10^{-9} mol cm^{-2} h^{-1}) of CH_4 reacting at low temperatures to form C_1 molecules, which Frese attributed to the increased lifetime of the intermediate species, possibly generated electrochemically by using a high pH solution.[32]

More recently, the electro-oxidation of CH_4 under low temperature conditions has been reported on Pd[33] and Pt/Ru alloys.[103] Hahn and Melendres used *in situ* infrared spectroscopy to monitor the electro-oxidation of CH_4 on Pd electrodes at room temperature in perchloric acid.[33] Their studies showed that –CO, –CHO, and –COOH were the intermediate species with the final oxidation product always being CO_2, regardless of the electrode material. The intermediate species produced suggest that there is some involvement of H_2O or OH$_{ads}$ in the reaction mechanism. Platinum and ruthenium appeared to be the most active of the electrodes. Zhang *et al.* proposed that using a roughened or smooth Pd electrode could produce CO_2 *via* 8-electron anodic oxidation of CH_4 under ambient conditions.[20] These studies were carried out using cyclic voltammetry between 0.0 to +1.5 V, multiple scan rates, and under varying CH_4 concentrations.[20] Based on the previous studies[33,67,104,105] and their own, they proposed electro-oxidation to be a multi-step process (the asterisk denotes adsorbed species):

$$CH_4 \rightarrow CH^*_{3(ads)} + H^+ + 1e^- \qquad (4)$$

$$CH^*_{3(ads)} + H_2O \rightarrow CO^*_{(ads)} + 5H^+ + 5e^- \qquad (5)$$

$$CO^*_{(ads)} + H_2O \rightarrow CO_2 + 2H^+ + 2e^- \qquad (6)$$

Overall anodic oxidation is then equal to

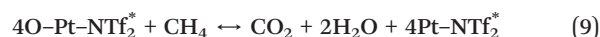$$CH_4 + 2H_2O \rightarrow CO_2 + 8H^+ + 8e^- \qquad (7)$$

This shows that CH_4 dissociates at the electrode surface to a CH_x species, which is then covered with CO through a

series of surface reactions that eventually leads to the formation of CO_2. Their multi-step process is similar to that reported by the other studies, where CO_2 and H^+ are the final products in the electro-oxidation. Additionally, they reported high electrocatalytic activity of the roughened electrode, as opposed to smooth Pd, which can possibly be attributed to a larger surface to volume ratio.[20] Recently, Wang and Zeng approached the activation of CH_4 using ionic liquids (ILs), which are organic electrolytes that contain charge-diffuse cations and anions with minimal vapor pressure and are stable under various experimental conditions.[23] ILs potentially increase solubility of CH_4 and provide a strong polar environment, presumably facilitating CH_4 activation electrostatically. Using bis(trifluoromethylsulfonyl)imide (NTf$_2$) based ILs, a Pt gauze working electrode pressed into a porous Teflon membrane and polycrystalline Pt wires as the counter and quasi-reference electrodes, the electro-oxidation of CH_4 was attempted. Experiments were performed at 25 °C in acidified electrolyte and the potentials scanned were from 1.5 V to −1.8 V.[23] Other working electrodes, such as gold and carbon, were also used to determine if CH_4 could be oxidized. Overall, CH_4 was fully oxidized to H_2O and CO_2 using NTf$_2$ based ILs at room temperature, but the results appeared to be dependent on the conditions under which the experiment is run (*i.e.* oxygen concentration, the potential of the electrode, and properties of the IL). Wang and Zeng proposed that adsorbed oxygen atoms on vacant Pt sites react with the ILs to form the stable complex

$$Pt\text{–}O + NTf_2^- \leftrightarrow O\text{–}Pt\text{–}NTf_2^- \leftrightarrow O\text{–}Pt\text{–}NTf_2^* + e \qquad (8)$$
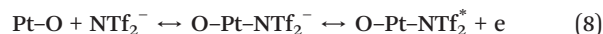
which then reacts with CH_4

$$4O\text{–}Pt\text{–}NTf_2^* + CH_4 \leftrightarrow CO_2 + 2H_2O + 4Pt\text{–}NTf_2^* \qquad (9)$$

so that the overall reaction proceeds as

$$CH_4 + O_2 \xrightarrow{Pt\text{–}NTf_2\text{–}IL} CO_2 + 2H_2O \qquad (10)$$

From the data discussed so far, it quickly becomes apparent that very few direct electrochemical oxidation processes lead to oxygenate intermediates that can be stabilized and isolated as liquid fuel or commodity chemical products. Mechanistic studies lead to the belief that the adsorbed species undergo further oxidation with fewer electrons than the number needed to activate CH_4 in the first place. Conventional catalytic processes proceed heterogeneously *via* gas–solid surface interactions and thus kinetics can be controlled rather easily by optimizing contact time; however, this is much more difficult to accomplish when using aqueous solutions. Furthermore, this process is further complicated by the presence of various indiscriminate radical species in solution, which nonselectively oxidize any carbon containing molecules formed.

2402 | *Catal. Sci. Technol.*, 2014, **4**, 2397–2411

This journal is © The Royal Society of Chemistry 2014

This problem is partially remedied when an indirect electrochemical CH_4 oxidation process is used. Ogura and Takamagari combined electrochemistry and photochemical oxidation of CH_4 using a 0.6 M KCl solution as an electrolyte to produce CH_3OH, CH_3Cl, and CH_2Cl_2.[49] The formation of the products greatly depended on the cell potential, which varied from 1.1 to 2.0 V at pH 11.0. In this seminal, yet underfollowed study, the combination of the two energy input methods produced a chlorine molecule, which then formed a radical; upon illumination, it further reacted with CH_4 to form photochemically chlorinated CH_4 or chloromethane (CH_3Cl), which in all cases appeared to be the dominant product. Methanol (CH_3OH) and dichloromethane (CH_3Cl_2) tended to be the next most common species present. The mechanism for the production of CH_4 was proposed via two methods. The first method involved the formation of a MOH species, where M is the electrode, which then proceeded to react with a methyl radical to produce methanol. The second method involved the hydrolysis of CH_3Cl to produce methanol and chloride ions. Both methods are thought to occur due to the observation of methanol production even at low pH (pH ~1). These studies were further refined by Ogura, et al.[47,48] Their investigation showed that using Pt working and counter electrodes at 1.3 V vs. the SHE produced CH_3OH, CH_3Cl, and CH_2Cl_2 in aqueous electrolyte at pH = 11.0 when illuminated for 3 hours with a 10 W Hg lamp at 25 °C. The major product observed was CH_3Cl, followed by either CH_2Cl_2 or CH_3OH, with a negligible amount of carbon tetrachloride (CCl_4) reported. The formation of CH_2Cl_2 and CH_3OH was determined to be dependent on the concentration of the chloride ion present in the electrolyte. The authors proposed that upon the photodissociation of Cl_2 at 350 nm, CH_4 can be converted to methyl chloride and methanol by electrochemical oxidation under illumination. The formation of methanol was proposed to be due to the hydrolysis of CH_3Cl, which was enhanced electrochemically. Ogura et al. then examined the photochemical activation of CH_4 in the presence of water which produced methanol as the dominant product (~70% at 90 °C) followed by formic acid (11%), ethanol (5%), formaldehyde (5%), acetone (4%) and acetic acid (3%). This was attributed to the hydroxyl radical formation from the photolysis of water at temperatures lower than 100 °C.[48] Clearly, the work demonstrated by Ogura et al. showed a powerful proof of concept of indirect CH_4 activation to liquid oxygenates at atmospheric pressure and temperature. It relied, however, on the inherent reactivity of ions in halide aqueous solutions, thus circumventing indiscriminate electron/reactive radical based complete CH_4 oxidation.

2.2. Photochemical CH_4 activation

Photochemical processes involve a semiconductor material excited with light to generate charge carrier pairs, e.g. electrons and holes. By analogy with the electrochemical process, these electrons can be used in reduction reactions as a substitute for thermal energy, whereas holes in the conduction band can perform oxidation. The resulting charge carriers possess kinetic energy equal to that of the bandgap of the semiconductor material and could possibly drive thermodynamically unfavorable ($\Delta G > 0$) CH_4 activation reactions. A simplistic view of this process is shown in Fig. 3 where the solar spectrum is shown with the specific CH_4 activation reactions of interest, converted to energy of one mole of photons. It quickly becomes apparent that, for example, theoretically CH_3OH formation can be driven on a photocatalyst using a semiconductor material with a bandgap of ~1000 nm (~1.3 eV). Practically, however, this will always be preceded by C–H bond breaking which requires much more energy (434 kJ mol^{-1} or 275 nm). It is expected that suitable photocatalysts in combination with a molecule reforming co-catalyst could drive these thermodynamically unfavorable reactions[106] resulting in the formation of storable energy dense chemicals or a storable form of solar energy.

A tutorial style review of photocatalytic CH_4 activation was published in 2008.[107] We will focus on the new developments in the methods and photocatalyst materials as well as the possible applied aspects of photocatalytic CH_4 activation.

2.2.1. Photocatalytic steam (aqueous) reforming. An emerging CH_4 activation method that utilizes the photocatalytic phenomenon – photocatalytic steam reforming of CH_4[108–110] – proceeds according to reaction (11)

$$CH_4 + 2H_2O \rightarrow 4H_2 + CO_2, \Delta G(298\ K) = 114\ kJ\ mol^{-1} \quad (11)$$

While this can be regarded as a combination of steam (although photocatalytically performed in aqueous medium, the steam reforming name is historically used) methane reforming and water gas shift reactions, the resulting H_2 is even more difficult to pressurize/liquefy than CH_4 and problematic to use as liquid fuel. Previous work in this area has mostly originated from Nagoya University and focused on noble metal cocatalyzed wide bandgap insulator systems, such as Pt/TiO$_2$,[111] Pt/CaTiO$_3$,[112] Pt/NaTaO$_3$:La,[108] Rh$_2$O$_3$/K$_2$Ti$_6$O$_{13}$,[110] Pt/β-Ga$_2$O$_3$,[113] and Pt,Rh,Au,Pd,Ni/β-Ga$_2$O$_3$.[114] Wide bandgap catalysts such as TiO$_2$ and β-Ga$_2$O$_3$ are well known in photocatalytic water splitting, although they require UV light. This results in stringent criteria for the overall process efficiency,
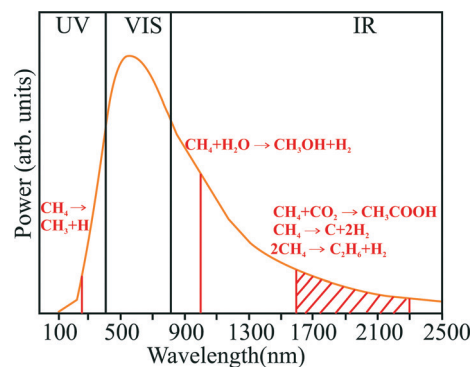

Fig. 3 The solar spectrum and energy requirement of several thermodynamically unfavorable CH_4 activation reactions.

This journal is © The Royal Society of Chemistry 2014

Catal. Sci. Technol., 2014, 4, 2397–2411 | 2403

if the visible spectrum is used. One of the first processes was carried out at room temperature and room pressure with an almost stoichiometric product mixture (4 : 1) on Pt/TiO_2.[111] Additionally, various catalyst structures and composition parameters were explored for $Pt/CaTiO_3$,[112] while substitutional doping of the photocatalyst material $Pt/NaTaO_3$:La[108] and the co-catalyst effect on Pt,Rh,Au,Pd,Ni/β-Ga_2O_3[114] were also explored. Noble metal catalysts have been shown to be necessary to improve generated charge carrier separation and to catalyze H_2 evolution and seem to be necessary for aqueous photocatalytic CH_4 reforming. However, Ni loaded onto β-Ga_2O_3 particles using *in situ* photodeposition showed reasonable H_2 production rates, comparable to those of the Pd or Au co-catalyst, while co-deposited Rh showed the best overall performance (0.4 μmol min^{-1}).[114] Nickel is a well-known CH_4 steam reforming catalyst, thus active in C–H bond breaking, and it has also recently been shown to be efficient as a non-noble hydrogen evolution catalyst in complexes such as nickel nitrides and phosphides, with the Ni_2P (001) surface being catalytically active.[115,116] Various nickel phosphides with crystalline phases have been shown to possess photocatalytic properties in oxidizing various organic compounds[117,118] and can be proposed to be used to improve photocatalytic steam reforming efficiency. Finally, small ions (Al^{3+}, Mg^{2+}, In^{3+}, and Zn^{2+}) doped into the β-Ga_2O_3 structure increased H_2 evolution activity,[114] which could possibly be due to improved photocatalytically generated charge carrier separation. While liquid fuels are not produced using this method, of great interest would be experiments where syngas is produced, rather than a H_2 + CO_2 mixture. However, to date the authors are unaware of any data reported on these attempts.
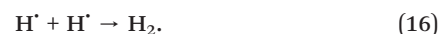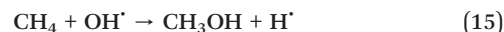
2.2.2. Partial photochemical CH_4 oxidation to methanol. Direct photocatalytic oxidation to CH_3OH *via* reaction (12) has been of perennial interest due to CH_3OH serving as an intermediate of a wide range of chemicals while a byproduct, H_2, is an energy carrier

$$CH_4 + H_2O \rightarrow CH_3OH + 4H_2, \Delta G(298\ K) = 117\ kJ\ mol^{-1} \quad (12)$$
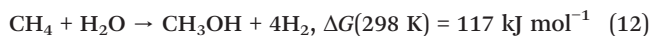
Initial attempts at oxidation have been made at the United States Department of Energy National Energy Technology Laboratory (DOE NETL) using CH_4[119,120] and methane hydrate[121] to produce CH_3OH using doped TiO_2 and WO_3 photocatalyst aqueous chemistry. Typical CH_4 conversion was ~4% on La/WO_3,[120] with 1.7 g of $CH_3OH\ g^{-1}$ of the catalyst h^{-1} produced.[122] Other products, in addition to those in reaction (12), were H_2, CO, and O_2,[120,122] proposed to be formed *via* H_2O photochemical splitting and the resulting radical chemistry. Co-catalysts other than La, such as Pt and Cu, resulted in equal or lower CH_3OH production than La. Experiments were performed at 95 °C and no CH_3OH was observed at temperatures <70 °C, implying that there is a thermal barrier. Simulated methane hydrate photocatalytic activation on both La/WO_3 and TiO_2 resulted in other products, such as C_2H_6, HCOOH and CO_2.[121] The difference from previous experiments was the use of high pressure (10 MPa) to induce

the formation of hydrates at 268 K before the reaction.[121] Since the latter experiment was performed in a batch mode for 1 h, these products, including CO_2, can be proposed to be kinetically controlled, as is typical in partial CH_4 oxidation reactions. The use of a high intensity coherent laser source in combination with TiO_2, WO_3 and NiO photocatalysts was explored to intensify the CH_3OH production process.[123,124] The laser wavelength used was greater than the bandgap of the corresponding material to ensure the photocatalytic phenomenon. The interplay between the photocatalyst loading (~0.07 g L^{-1}) and the laser power (1.5 W) always resulted in a maximum on the CH_3OH concentration curve, defining the optimal photocatalytic conditions.[123]

Mechanistically, several free radical based transformations occur with a hydroxyl radical proposed as a key intermediate[121,122,124]

$$SC + h\nu \rightarrow SC\ (h_{VB}^+, e_{CB}^-) \quad (13)$$

$$H_2O + h_{VB}^+ \rightarrow H^\cdot + OH^\cdot \quad (14)$$

$$CH_4 + OH^\cdot \rightarrow CH_3OH + H^\cdot \quad (15)$$

$$H^\cdot + H^\cdot \rightarrow H_2. \quad (16)$$

However, CH_3OH produced can further react with holes or a superoxide radical produced either from dissolved O_2 or that generated *via* photocatalytic H_2O splitting, yielding HCOOH, CO and CO_2. This presents a selectivity challenge, as O_2 evolution from H_2O must be inhibited for the process to be CO_2 neutral. This presents an opportunity to use ionic liquids that dissolve CH_4 at rates higher than H_2O, which is also a prerequisite for any photoelectrochemical process. Conventional catalysis has been successfully attempted to directly convert CH_4 to CH_3OH in ionic liquids on Pt based catalysts[125–127] providing the lead here.

2.2.3. Non-oxidative photocatalytic CH_4 coupling. Direct photocatalytic CH_4 coupling to yield ethane proceeds *via*

$$2CH_4 \rightarrow C_2H_6 + H_2, \Delta G(298\ K) = 68.6\ kJ\ mol^{-1}. \quad (17)$$

Many photocatalyst materials explored thus far are largely based on transition metal substituted silica framework materials, as will be discussed below.

2.2.3.1. Wide bandgap photocatalysts. Wide bandgap photocatalysts have been extensively used for this purpose so far, even though they absorb only a fraction of the incident solar radiation spectrum. Room temperature experiments on ethane and H_2 production were performed using a silica matrix with incorporated noble metal ions *via* Si–O–M linkage, where M is Zn,[128] Ce,[129] Ti,[130] Ga,[131] Al,[132] Zr,[133] and Mg.[133] Ce was shown to be the only active metal ion with a detectable efficiency out of the 14 tested rare earth dopants incorporated into the silica matrix.[129] Interesting synergistic effects within ternary compounds, such as SiO_2–Al_2O_3–TiO_2, have been observed[130] with the increase in C_2H_6 and even the C_3H_8

2404 | Catal. Sci. Technol., 2014, 4, 2397–2411

This journal is © The Royal Society of Chemistry 2014

product yield over those of the binary compounds. A CH_4 conversion rate of 9.8 $\mu mol\ g^{-1}$ of the catalyst h^{-1} was reported for Zn doped ZSM-5 irradiated with a high pressure Hg lamp with selectivity greater than 99% for ethane and hydrogen products.[128] Incorporation of other metals, such as Ga, Al, Zn and Fe into ETS-10 (*e.g.* a microporous titanosilicate framework) resulted in an enhanced CH_4 conversion rate of 29.8 $\mu mol\ g^{-1}$ of the catalyst h^{-1} for the best performing Ga dopant.[131] Remarkably high selectivities towards ethane and hydrogen were observed in photocatalytic experiments using ZSM-5 as a host (99%)[128] allowing the use of the shape selectivity argument in the framework of photocatalytic CH_4 coupling.

Any CH_4 activation has to proceed *via* initial C–H bond breaking and any photocatalytic mechanisms or catalysts that facilitate this can be proposed to enhance the conversion rate. High activity of certain metal oxides in H/D exchange and C–H bond dissociation experiments has been classified for Cr_2O_3, Ga_2O_3 and ZnO, with MgO and some rare earth metal oxides showing moderate activity.[134] MgO dispersed within SiO_2 has been shown to yield ~0.03% hydrocarbons due to the Si–O–Mg linkage sites.[135] While not explicitly mentioned, MgO could have synergistically acted as a C–H bond dissociation cocatalyst, as confirmed by high efficiencies of Mg, Ga and Zn doped silica materials.[128,131] An additional photocatalytic reaction parameter that could impact the activity of CH_4 is increasing the temperature, which has been shown to double the amount of C_2H_6 and H_2 produced on β-Ga_2O_3 with an increase in temperature from 314 to 473 K.[107] This was suggested to be due to the enhanced desorption of reaction intermediates and products or the enhanced migration of photoexcited electrons. There was, however, a non-stoichiometric amount of products generated with excess H_2 pointing towards several competing reactions proceeding at different rates at elevated temperatures. Notably, we could not find any mention of the formation of a CO_x product using photocatalytic coupling reactions[133] on any of these metal oxide photocatalyst surfaces suggesting that the process is potentially CO_2 neutral and most likely proceeds *via* Si–O˙ radical and charge transfer induced photochemistry[135] and is not a Mars–van Krevelen type of reaction.

A special case of CH_4 activation using a combination of deep UV (180–200 nm) and solid surfaces containing hydroxyl groups was performed by Corma and García's group.[136,137] C_1 oxygenates were obtained with CH_4 conversion of up to 7% *via* indirect hydroxyl radical based C–H bond breaking. H_2 accounted for ~50% of the products with C_2H_5OH accounting for ~26% using a beta zeolite after 11 hours of irradiation at room temperature. When O_2 was present as a co-reactant, the oxygenated product selectivity was 95%. Analogously, a theoretical study on CH_4 activation on the external radical generating reactant, H_2S, has been shown to yield reactive HS˙ and H˙ radicals in the presence of 200 nm light to reform CH_4 into CH_3SH, an activated CH_4 intermediate.[138] The latter process, albeit only theoretically investigated, allows for the conversion of the so-called "sour" natural gas which accounts for ~40% of the available conventional resources.

These types of processes again are heavily reliant on *in situ* radical generation and can be envisioned to take place in UV lamp equipped reactors where surplus electricity is present.

2.2.3.2. Visible bandgap photocatalysts. An intuitive approach to photocatalytic transformations suggests that better solar utilization efficiency can be achieved if photocatalyst materials can absorb visible light, thus utilizing most of the incident spectrum. Data reported by Li *et al.* on CH_4 photocatalytic coupling using Zn^+-SiO_2[128] yielded 24% CH_4 conversion upon irradiation of the catalyst for 8 hours using a high-pressure mercury lamp. Furthermore, this photocatalyst has been shown to be active upon irradiation with visible light, although the reaction rate decreased and conversion stopped after 8 hours. The electron transfer process, as inferred from Electron Paramagnetic Resonance (EPR) spectroscopy, must proceed initially from the zeolitic framework to the 4s orbital of Zn^{2+} upon UV irradiation at wavelengths less than 390 nm while visible light (~700 nm) is utilized to cocatalyze the Zn 4s electron to the C–H σ^* antibonding orbital of CH_4, thus activating CH_4 to form C_2H_6 and H_2 (Fig. 4).[128] Due to the UV energy utilized in the first step, the zeolitic materials will possess low visible light efficiency. An attractive concept here would be visible light-absorbing materials, possessing unsaturated oxygen atoms that could act as radical centers. While small clusters of similar materials have only been observed in the gas phase and are not yet applicable in applied heterogeneous catalysis, the oxygen-centered radical concept for CH_4 activation can provide the necessary leads.[139] The spin density localized on oxygen atoms is capable of a nearly barrier-free gas phase CH_4–hydrogen atom transfer and the mechanisms have been investigated extensively using DFT in a multitude of transition metal clusters.[139–141] By analogy, polyoxometalates (POMs) possess terminal oxygen atoms which are active sites for photocatalytic oxidation reactions[142] *via* oxygen localized radicals.[143] They have already been shown to be active in
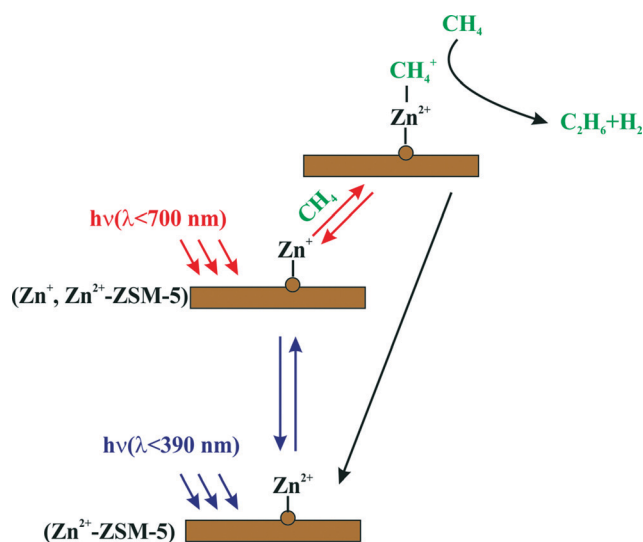

Fig. 4 CH_4 activation on Zn^+-SiO_2 using visible light, adapted from Li *et al.*[128]

This journal is © The Royal Society of Chemistry 2014

Catal. Sci. Technol., 2014, **4**, 2397–2411 | **2405**

thermal CH_4 activation.[144] Furthermore, ample POMs have currently been synthesized that absorb visible light and possess terminal oxygen groups which can act as radical carriers upon photoexcitation,[145] thus potentially serving as visible light operated CH_4 activation catalysts.

Lastly, chlorine radical mediated photocatalytic C–H bond activation on a TiO_2/BiOBr photocatalyst has been shown to proceed under visible light ($420 < \lambda < 780$ nm) irradiation in the presence of 1 atm oxygen at room temperature with remarkable selectivities (>85%).[146] Chlorine radicals formed on a photocatalyst surface, due to excess co-adsorbed oxygen and CH_4, do not form alkyl halides but rather oxygenated compounds. This is akin to homogenous phase halogen based CH_4 activation reactions that suffer from poor selectivity due to the higher number of degrees of freedom of the chlorine radicals generated. This process potentially offers a new photocatalytic route for C–H bond activation at room temperature utilizing visible light as the sole energy source. The high selectivity reported implies a CO_2 neutral process as no byproducts, other than minor HCl and O_2, have been reported.[146]

2.2.3. Dry (carbon dioxide) photocatalytic reforming of CH_4. Dry (carbon dioxide) photocatalytic reforming of CH_4 proceeds *via*

$$CH_4 + CO_2 \rightarrow 2CO + 2H_2, \Delta G(298\ K) = 171\ kJ\ mol^{-1} \quad (18)$$
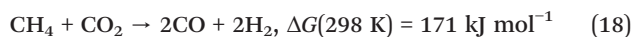
Wide bandgap semiconductors have been used to overcome the large activation barrier photochemically using β-Ga_2O_3,[107] Cu/CdS–TiO_2/SiO_2,[147] ZrO_2,[148,149] ZnO,[150] TiO_2[151] and copper phthalocyanine modified TiO_2[152] on a stainless steel mesh, as well as on MgO.[153] A more interesting alternative is the potential of direct C–C coupling of CH_4 and CO_2 to acetic acid (CH_3COOH ($\Delta G(298\ K) = 71.1\ kJ\ mol^{-1}$)), acetone ($CH_3COCH_3$ ($\Delta G(298\ K) = 115\ kJ\ mol^{-1}$)) or other related compounds. Photocatalytic reforming data are summarized in Table 2.

It can be seen that the catalyst used as well as the temperature of the photocatalytic reaction affected the product selectivity.

Cu/CdS–TiO_2/SiO_2 was shown to be selective towards CH_3COCH_3 formation at 393 K, whereas β-Ga_2O_3 yielded primarily C_2H_6. Additional products that were observed but not quantified were oxalic acid, acetaldehyde, acetic acid, water, and CO,[152] although in this particular case it's not clear whether copper phthalocyanine itself didn't decompose. A thermal effect was apparent and can also be seen from the data presented in Table 2. CH_4 and CO_2 conversion increased with temperature, but at higher temperatures a noticeable amount of CO and excess H_2 were observed, possibly suggesting that reforming reactions become more favorable over coupling. Low temperatures favored high selectivity of 83% towards C_2H_6.[107] Only in one case was the gas hourly space volume (GHSV) reported to be 200 h^{-1} whereas other batch experiments were carried out for 1–8 hours. Finally, the process and the catalyst for CH_4 + CO_2 photochemical reforming on non-metal oxides – transition metal chalcogenide photocatalysts – in a recent patent application[154] were claimed, including an example of RuS_2 in a UV light reactor with a CH_4:CO_2 (50%:50%) stream, to produce an unspecified mixture of paraffins, olefins and alcohols. Conceptually, certain transition metal sulfides (CoS, RuS_2, NiS, MoS_2 and WS_2) have a bandgap of 1.1 to 1.8 eV (1130 to 690 nm) thus absorbing visible radiation[138] but the reaction mechanism is not immediately clear.

3. Limitations and future applications of renewable energy based CH_4 conversion

Electrons and holes needed to perform CH_4 conversion can be delivered directly with solar light or in the form of electricity. Electrochemistry can lead to much faster conversion rates, and hence more intense processes, especially since at low temperatures it can borrow fundamental and applied knowledge from the well-established water electrolysis technology. A clear advantage of the electrochemical process, when compared with the conventional heterogeneous catalysts, is that in most cases no catalyst preparation is necessary, unlike CH_4

Table 2 Dry photocatalytic reforming of CH_4[a]

Temperature, K	Conversion, %		Selectivity, %				
	CH_4	CO_2	CH_3COOH	C_2H_6	CH_3COCH_3	CO	H_2
303 (ref. 147)	0	0.0	—	—	—	—	N/A
353 (ref. 147)	0.11	0.07	—	46.7	0	53.3	N/A
393 (ref. 147)	1.47	0.74	Trace	3.1	92.3	4.6	N/A
423 (ref. 147)	1.54	0.79	Trace	7.5	87.6	4.9	N/A
298 (ref. 150)	15.83	12.35	—	—	—	—	—
333 (ref. 151)	33.1	27.9	—	—	—	—	—
298 (ref. 152)	18	14	—	—	—	—	—
314 (ref. 107)	—	—	—	83	—	—	—

[a] Reaction conditions: Shi *et al.*:[147] Cu/CdS–TiO_2/SiO_2, 1 atm, CO_2:CH_4 (50% CO_2:50% CH_4), UV light, 20.0 mW cm^{-2}, GHSV 200 h^{-1}; Mahmodi *et al.*:[150] 8 g of ZnO (2.65 mg cm^{-2}), 2 atm, (10% CO_2:80% CH_4:10% He) and a UV light source of 250 W; Merajin *et al.*:[151] TiO_2, 4 atm (45% CO_2:45% CH_4:10% He), a UV light source of 125 W, 8 h; Yazdanpour *et al.*:[152] 1 g of copper phthalocyanine/TiO_2, 4 atm (45% CO_2:45% CH_4:10% He), a visible light source of 125 W, 3 h; Yuliati *et al.*:[107] 0.2 g of β-Ga_2O_3, a 300 W UV light source with 9 mW cm^{-1}, 3 h. The room temperatures assumed were not reported.

steam reformers, where catalyst reduction must proceed initially. Additionally, the electrochemical process can be used in combination with the current PV or wind technology to limit the use of fossil fuels used during the CH_4 activation. Effectively, this allows for electrochemical CH_4 activation to start almost instantaneously whenever excess electricity is present. This can be considered advantageous compared to small scale CH_4 steam reforming where the startup time still needs to be improved.[155] The data reviewed, however, present very few opportunities for electrochemical CH_4 activation at low temperatures due to the low selectivity and slow rate of the process. A notable exception is based on aqueous halide solution electrochemistry to generate methanol and methyl halides.[49] This can be viewed as a low temperature alternative to the recent efforts devoted to halogen based CH_4 conversion to liquid fuels.[1,156,157]

A summary of the photocatalytic CH_4 activation is shown in Fig. 5. As typical for solar energy utilization, the achievable rate is limited by the photon flux of the sun. This in turn requires expansion of the photoreactor area. Naturally, the process cannot be continuous throughout the day because of limited illumination time in a day and its lack thereof at night. Furthermore, the somewhat low efficiency of charge separation of the photocatalytic process coincides with the difficult adsorption process of the reactant (CH_4), which is

essential for the activation reaction. Most of the reported photocatalysts are strongly limited by the UV-responsive materials. Thermodynamic requirements (band positions) for the photocatalysts are additional requirements to ensure that the desired reactions proceed. Somewhat unexpectedly, photocatalysis provides for a much better selectivity to the products. These processes could potentially proceed at room temperature, where, for example, CH_4 coupling reactions are thermodynamically favored;[138] the energy supplied from photons is also used to overcome C–H bond activation, normally an endothermic process, while high temperatures provide thermodynamic stability for solid carbon formation[158] and the resulting loss of catalyst activity.

However, the overall process efficiency remains an issue for the photochemical processes. From the literature reviewed, a GHSV of only 200 h^{-1} was achieved[147] with the rest of the experiments run in a batch mode. This is unlike the catalytic oxidative CH_4 coupling where the GHSV is orders of magnitude higher (8000–17 000 h^{-1}).[159] Nevertheless, photochemical CH_4 activation provides excellent opportunities in combining light and temperature effects at the same time since it can also be performed in the gas phase as well as in solution. Finally, conceptually new combined catalytic processes can be envisioned. For example, dry conventional CH_4 reforming results in a nonstoichiometric syngas mixture on Ni, Ru, Rh/Al_2O_3
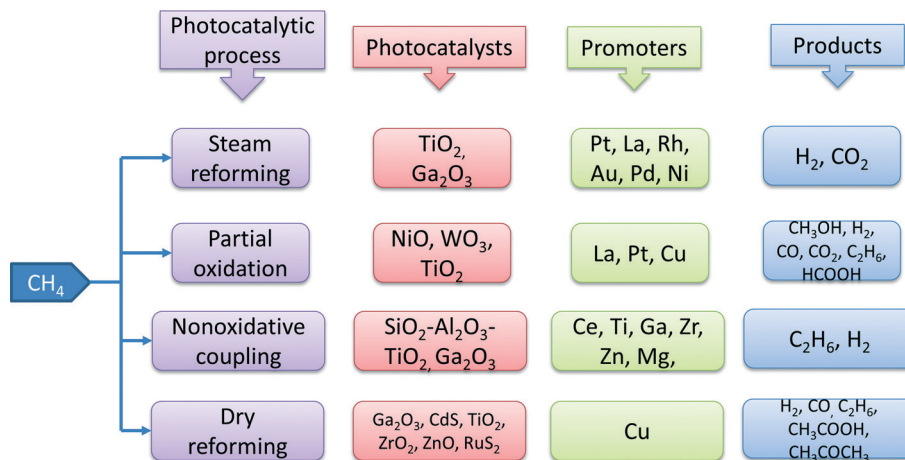

Fig. 5   The photocatalytic process, catalyst and co-catalyst materials and observed products in the photocatalytic CH_4 activation.
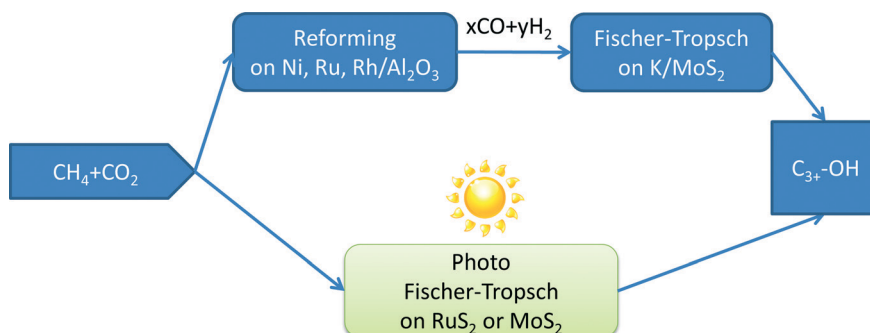

Fig. 6   A conceptual "photo-Fischer–Tropsch" synthesis of higher alcohols from CH_4 + CO_2.

This journal is © The Royal Society of Chemistry 2014

Catal. Sci. Technol., 2014, 4, 2397–2411 | 2407

or SiO_2[160] which can be later used to produce C_1–C_5 hydrocarbons *via* the Fischer–Tropsch process (Fig. 6). A class of alkali cocatalyzed molybdenum, nickel or cobalt sulfide catalysts has emerged to produce higher alcohols from syngas.[161–163] Metal sulfides are well-known photocatalysts and recently have become widely utilized in photochemical H_2 evolution from H_2O.[164] Conceptually, the photochemical effect can be envisioned to combine both syngas production and the resulting alcohol forming reactions on metal sulfide photocatalysts, in agreement with the recently filed patent.[154]

4. Conclusions

Based on the analyses provided above, we have identified the key opportunities & technical challenges that photoelectrochemical approaches present *vs.* conventional thermochemical routes. The idea to use photoelectrochemisty for CH_4 processing into liquid fuels is synergistically driven: both CH_4 and electricity are difficult to store or transport. Using the combination of photons and electricity may tell us whether or not these processes have a chance to compete for large scale applications, for fuel or rather chemicals, or whether we should seek opportunities in smaller scale, niche applications.

Acknowledgements

References

1 E. McFarland, *Science*, 2012, **338**, 340–342.
2 Washington, DC, *U.S. Energy Information Administration, Proved Reserves of Natural Gas - International Energy Statistics*, 2013.
3 W. Liss, *Chem. Eng. Prog.*, 2012, **108**, 34.
4 Y. Chang, X. Liu and P. Christie, *Environ. Sci. Technol.*, 2012, **46**, 12281–12282.
5 J. N. Armor, *J. Energy Chem.*, 2013, **22**, 21–26.
6 G. J. Moridis, T. S. Collett, R. Boswell, M. Kurihara, M. T. Reagan, C. Koh and E. D. Sloan, *SPE Reservoir Eval. Eng.*, 2009, **12**, 745–771.
7 J. J. Spivey and G. Hutchings, *Chem. Soc. Rev.*, 2014, **43**, 792–803.
8 L. Luo, X. Tang, W. Wang, Y. Wang, S. Sun, F. Qi and W. Huang, *Sci. Rep.*, 2013, **3**, 1625, DOI: 10.1038/srep01625.
9 B. Christian Enger, R. Lødeng and A. Holmen, *Appl. Catal., A*, 2008, **346**, 1–27.
10 Q. Zhu, S. L. Wegener, C. Xie, O. Uche, M. Neurock and T. J. Marks, *Nat. Chem.*, 2013, **5**, 104–109.
11 C. Hammond, S. Conrad and I. Hermans, *ChemSusChem*, 2012, **5**, 1668–1686.
12 S. Abelló and D. Montané, *ChemSusChem*, 2011, **4**, 1538–1556.
13 J. P. Lange, K. P. de Jong, J. Ansorge and P. J. A. Tijm, *Stud. Surf. Sci. Catal.*, 1997, **107**, 81–86.
14 Z. Chen, T. F. Jaramillo, T. G. Deutsch, A. Kleiman-Shwarsctein, A. J. Forman, N. Gaillard, R. Garland, K. Takanabe, C. Heske,

M. Sunkara, E. W. McFarland, K. Domen, E. L. Miller, J. A. Turner and H. N. Dinh, *J. Mater. Res.*, 2010, **25**, 3–16, DOI: 10.1557/JMR.2010.0020.
15 N. S. Lewis and D. G. Nocera, *Proc. Natl. Acad. Sci. U. S. A.*, 2006, **103**, 15729–15735.
16 Q. Schiermeier, *Nature*, 2013, **496**, 156–158.
17 R. Lan, J. T. S. Irvine and S. Tao, *Int. J. Hydrogen Energy*, 2012, **37**, 1482–1494.
18 *U.S. Energy Information Administration, Technically Recoverable Shale Oil and Shale Gas Resources: An Assessment of 137 Shale Formations in 41 Countries Outside the United States*, Washington, DC, 2013.
19 *SolarGIS © GeoModel Solar*, http://solargis.info/doc/71, accessed January 2014.
20 Y. Zhang, L. Zhang, S. Shuang, F. Feng, J. Qiao, Y. Guo, M. M. F. Choi and C. Dong, *Anal. Lett.*, 2010, **43**, 1055–1065.
21 K. Takanabe, *J. Jpn. Pet. Inst.*, 2012, **55**, 1–12.
22 R. A. Periana, O. Mironov, D. Taube, G. Bhalla and C. Jones, *Science*, 2003, **301**, 814–818.
23 Z. Wang and X. Zeng, *J. Electrochem. Soc.*, 2013, **160**, H604–H611.
24 D. A. Hickman and L. D. Schmidt, *Science*, 1993, **259**, 343–346.
25 S. C. Roy, O. K. Varghese, M. Paulose and C. A. Grimes, *ACS Nano*, 2010, **4**, 1259–1278.
26 Y. Amenomiya, V. I. Birss, M. Goledzinowski, J. Galuszka and A. R. Sanger, *Catal. Rev. Sci. Eng.*, 1990, **32**, 163–227.
27 E. J. Cairns, in *Advances in electrochemistry and electrochemical engineering*, ed. P. Delahay and C. W. Tobias, Wiley Interscience, New York, 1971, ch. 5, vol. 8, pp. 337–392.
28 D. Eng and M. Stoukides, *Catal. Rev. Sci. Eng.*, 1991, **33**, 375–412.
29 C. Athanasiou, G. Marnellos, P. Tsiakaras and M. Stoukides, *Ionics*, 1996, **2**, 353–360.
30 M. Stoukides, *J. Appl. Electrochem.*, 1995, **25**, 899–912.
31 I. Garagounis, V. Kyriakou, C. Anagnostou, V. Bourganis, I. Papachristou and M. Stoukides, *Ind. Eng. Chem. Res.*, 2010, **50**, 431–472.
32 K. W. Frese, *Langmuir*, 1991, 7, 13–15.
33 F. Hahn and C. A. Melendres, *Electrochim. Acta*, 2001, **46**, 3525–3534.
34 P. Jacquinot, B. Muller, B. Wehrli and P. C. Hauser, *Anal. Chim. Acta*, 2001, **432**, 1–10.
35 A. A. Yaremchenko, V. V. Kharton, A. A. Valente, E. V. Frolova, M. I. Ivanovskaya, A. V. Kovalevsky, F. M. B. Marques and J. Rocha, *Catal. Lett.*, 2006, **112**, 19–26.
36 S. F. Au, L. Blum, A. Dengel, B. Groβ, L. G. J. d. Haart, K. Kimmerle and M. Wolf, *J. Power Sources*, 2005, **145**, 582–587.
37 T.-J. Huang and J.-F. Li, *J. Power Sources*, 2007, **173**, 959–964.
38 H. D. Gesser and N. R. Hunter, *Catal. Today*, 1998, **42**, 183–189.
39 T. V. Choudhary, A. E. Aksoylu and D. W. Goodman, *Catal. Rev. Sci. Eng.*, 2003, **45**, 151–203.
40 A. Katsaounis, *J. Appl. Electrochem.*, 2010, **40**, 885–902.

41 D. Lance and E. G. Elworthy, *French Patent*, 1905, 352 687.

42 R. Schonfelder, *Ber. Ges. Kohlentech.*, 1923, (iv), 247–263.

43 P. L. Fabre, J. Devynck and B. Tremillon, *Tetrahedron*, 1982, **38**, 2697–2701.

44 T. Otagawa, S. Zaromb and J. R. Stetter, *J. Electrochem. Soc.*, 1985, **132**, 2951–2957.

45 H. P. Fritz and T. Würminghausen, *J. Electroanal. Chem. Interfacial Electrochem.*, 1974, **54**, 181–187.

46 J. Cassidy, S. B. Khoo, S. Pons and M. Fleischmann, *J. Phys. Chem.*, 1985, **89**, 3933–3935.

47 K. Ogura and M. Kataoka, *J. Mol. Catal.*, 1988, **43**, 371–379.

48 K. Ogura, C. T. Migita and Y. Ito, *J. Electrochem. Soc.*, 1990, **137**, 500–503.

49 K. Ogura and K. Takamagari, *Nature*, 1986, **319**, 308–308.

50 R. L. Cook and A. F. Sammells, *J. Electrochem. Soc.*, 1990, **137**, 2007–2008.

51 L. W. Niedrach, *J. Electrochem. Soc.*, 1964, **114**, 17.

52 P. Sidheswaran, *J. Electrochem. Soc. India*, 1979, **28**, 271.

53 H. Binder, A. Köhling and G. Sandstede, *Rev. Energie Prim.*, 1965, **1**, 48.

54 H. Binder, A. Köhling and G. Sandstede, *Adv. Energy Convers.*, 1966, **6**, 135–148.

55 L. W. Niedrach and T. M, *J. Electrochem. Soc.*, 1967, **114**, 17.

56 A. Parmaliana, F. Frusteri, F. Arena and N. Giordano, *Catal. Lett.*, 1992, **12**, 353–360.

57 L. W. Niedrach, *J. Electrochem. Soc.*, 1966, **113**, 645–650.

58 E. A. Kolyadko, V. Menyailova and V. I. Podlovchenko, *Elektrokhimiya*, 1977, **13**, 273.

59 S. Y. Hsieh and K. M. Chen, *J. Electrochem. Soc.*, 1977, **124**, 1171–1174.

60 M. G. Sustersic, R. Córdova O., W. E. Triaca and A. J. Arvía, *J. Electrochem. Soc.*, 1980, **127**, 1242–1248.

61 A. M. Castro Luna, A. Delgado and A. J. Arvia, *An. Asoc. Quim. Argent.*, 1981, **69**, 301.

62 M. Bonnemay, G. Bronoel, D. Doniat and J. P. Peasand, *Fundamental study of adsorption of hydrocarbons on platinum electrode,* presented in part at the American Chemical Society, 1969.

63 A. A. Adams and R. T. Foley, *J. Electrochem. Soc.*, 1979, **126**, 775–778.

64 G. R. Schoofs, C. R. Arumainayagam, M. C. McMaster and R. J. Madix, *Surf. Sci.*, 1989, **215**, 1–28.

65 A. G. Sault and D. W. Goodman, in *Molecule-Surface Interactions*, ed. K. Lawley, John Wiley & Sons, England, 1989, vol. LXXVI, pp. 153–210.

66 F. Viñes, Y. Lykhach, T. Staudt, M. P. A. Lorenz, C. Papp, H.-P. Steinrück, J. Libuda, K. M. Neyman and A. Görling, *Chem. – Eur. J.*, 2010, **16**, 6530–6539.

67 G. Psofogiannakis, A. St-Amant and M. Ternan, *J. Phys. Chem. B*, 2006, **110**, 24593–24605.

68 R. G. Zhang, L. Z. Song and Y. H. Wang, *Appl. Surf. Sci.*, 2012, **258**, 7154–7160.

69 Y. Chen and D. G. Vlachos, *Ind. Eng. Chem. Res.*, 2012, **51**, 12244–12252.

70 S. Nave and B. Jackson, *J. Chem. Phys.*, 2009, **130**, 054701.

71 S. Nave, A. K. Tiwari and B. Jackson, *J. Chem. Phys.*, 2010, **132**, 054705.

72 H. L. Abbott and I. Harrison, *J. Catal.*, 2008, **254**, 27–38.

73 A. T. Anghel, D. J. Wales, S. J. Jenkins and D. A. King, *Chem. Phys. Lett.*, 2005, **413**, 289–293.

74 C. T. Au, C. F. Ng and M. S. Liao, *J. Catal.*, 1999, **185**, 12–22.

75 D. W. Blaylock, T. Ogura, W. H. Green and G. J. O. Beran, *J. Phys. Chem. C*, 2009, **113**, 4898–4908.

76 B. S. Bunnik and G. J. Kramer, *J. Catal.*, 2006, **242**, 309–318.

77 H. Burghgraef, A. P. J. Jansen and R. A. Vansanten, *Surf. Sci.*, 1995, **324**, 345–356.

78 I. M. Ciobica, F. Frechard, R. A. van Santen, A. W. Kleyn and J. Hafner, *Chem. Phys. Lett.*, 1999, **311**, 185–192.

79 I. M. Ciobica, F. Frechard, R. A. van Santen, A. W. Kleyn and J. Hafner, *J. Phys. Chem. B*, 2000, **104**, 3364–3369.

80 I. M. Ciobica and R. A. van Santen, *J. Phys. Chem. B*, 2002, **106**, 6200–6205.

81 K. M. DeWitt, L. Valadez, H. L. Abbott, K. W. Kolasinski and I. Harrison, *J. Phys. Chem. B*, 2006, **110**, 6705–6713.

82 A. Dianat, N. Seriani, L. C. Ciacchi, W. Pompe, G. Cuniberti and M. Bobeth, *J. Phys. Chem. C*, 2009, **113**, 21097–21105.

83 M. F. Haroun, P. S. Moussounda and P. Legare, *J. Mol. Struct.: THEOCHEM*, 2009, **903**, 83–88.

84 G. Henkelman and H. Jonsson, *Phys. Rev. Lett.*, 2001, **86**, 664–667.

85 T. Jacob and W. A. Goddard, *J. Phys. Chem. B*, 2005, **109**, 297–311.

86 A. Kokalj, N. Bonini, C. Sbraccia, S. de Gironcoli and S. Baroni, *J. Am. Chem. Soc.*, 2004, **126**, 16732–16733.

87 M. S. Liao and Q. E. Zhang, *J. Mol. Catal. A: Chem.*, 1998, **136**, 185–194.

88 H. Liu, R. Zhang, R. Yan, B. Wang and K. Xie, *Appl. Surf. Sci.*, 2011, **257**, 8955–8964.

89 A. C. Luntz and D. S. Bethune, *J. Chem. Phys.*, 1989, **90**, 1274–1280.

90 J. W. Medlin and M. D. Allendorf, *J. Phys. Chem. B*, 2003, **107**, 217–223.

91 P. S. Moussounda, M. F. Haroun, G. Rakotovelo and P. Legare, *Surf. Sci.*, 2007, **601**, 3697–3701.

92 G. Papoian, J. K. Norskov and R. Hoffmann, *J. Am. Chem. Soc.*, 2000, **122**, 4129–4144.

93 J. F. Paul and P. Sautet, *J. Phys. Chem. B*, 1998, **102**, 1578–1585.

94 M. A. Petersen, S. J. Jenkins and D. A. King, *J. Phys. Chem. B*, 2004, **108**, 5909–5919.

95 M. A. Petersen, S. J. Jenkins and D. A. King, *J. Phys. Chem. B*, 2004, **108**, 5920–5929.

96 V. A. Ukraintsev and I. Harrison, *J. Chem. Phys.*, 1994, **101**, 1564–1581.

97 S.-G. Wang, D.-B. Cao, Y.-W. Li, J. Wang and H. Hao, *Surf. Sci.*, 2006, **600**, 3226–3234.

98 L. Xiao and L. Wang, *J. Phys. Chem. B*, 2007, **111**, 1657–1663.

99 C. J. Zhang and P. Hu, *J. Chem. Phys.*, 2002, **116**, 322–327.

100 Y.-A. Zhu, D. Chen, X.-G. Zhou and W.-K. Yuan, *Catal. Today*, 2009, **148**, 260–267.

This journal is © The Royal Society of Chemistry 2014

Catal. Sci. Technol., 2014, **4**, 2397–2411 | **2409**

101 Z. Zuo, W. Huang, P. Han and Z. Li, *Appl. Surf. Sci.*, 2010, **256**, 5929–5934.

102 V. S. Bagotzky, Y. B. Vassiliev and O. A. Khazova, *J. Electroanal. Chem.*, 1977, **81**, 229–238.

103 H. A. Gasteiger, N. Markovic, P. N. Ross and E. J. Cairns, *J. Phys. Chem.*, 1993, **97**, 12020–12029.

104 A. B. Mhadeshwar and D. G. Vlachos, *Ind. Eng. Chem. Res.*, 2007, **46**, 5310–5324.

105 J. O. M. Bockris, E. Gileadi and G. E. Stoner, *J. Phys. Chem.*, 1969, **73**, 427–434.

106 L. Yuliati and H. Yoshida, *Chem. Soc. Rev.*, 2008, **37**, 1592–1602.

107 L. Yuliati, H. Itoh and H. Yoshida, *Chem. Phys. Lett.*, 2008, **452**, 178–182.

108 H. Yoshida, S. Kato, K. Hirao, J.-I. Nishimoto and T. Hattori, *Chem. Lett.*, 2007, **36**, 430–431.

109 K. Shimura, S. Kato, T. Yoshida, H. Itoh, T. Hattori and H. Yoshida, *J. Phys. Chem. C*, 2010, **114**, 3493–3503.

110 K. Shimura, H. Kawai, T. Yoshida and H. Yoshida, *ACS Catal.*, 2012, **2**, 2126–2134.

111 H. Yoshida, K. Hirao, J.-I. Nishimoto, K. Shimura, S. Kato, H. Itoh and T. Hattori, *J. Phys. Chem. C*, 2008, **112**, 5542–5551.

112 K. Shimura and H. Yoshida, *Energy Environ. Sci.*, 2010, **3**, 615–617.

113 K. Shimura, K. Maeda and H. Yoshida, *J. Phys. Chem. C*, 2011, **115**, 9041–9047.

114 K. Shimura, T. Yoshida and H. Yoshida, *J. Phys. Chem. C*, 2010, **114**, 11466–11474.

115 E. J. Popczun, J. R. McKone, C. G. Read, A. J. Biacchi, A. M. Wiltrout, N. S. Lewis and R. E. Schaak, *J. Am. Chem. Soc.*, 2013, **135**, 9267–9270.

116 W.-F. Chen, K. Sasaki, C. Ma, A. I. Frenkel, N. Marinkovic, J. T. Muckerman, Y. Zhu and R. R. Adzic, *Angew. Chem., Int. Ed.*, 2012, **51**, 6131–6135.

117 Y. Ni, L. Jin and J. Hong, *Nanoscale*, 2011, **3**, 196–200.

118 J. Li, Y. Ni, K. Liao and J. Hong, *J. Colloid Interface Sci.*, 2009, **332**, 231–236.

119 C. E. Taylor, R. P. Noceti and J. P. Deste, *Abstr. Pap. Am. Chem. Soc.*, 1995, **210**, 80.

120 R. P. Noceti, C. E. Taylor and J. R. Deste, *Catal. Today*, 1997, **33**, 199–204.

121 C. E. Taylor, *Top. Catal.*, 2005, **32**, 179–184.

122 C. E. Taylor and R. P. Noceti, *Catal. Today*, 2000, **55**, 259–267.

123 M. A. Gondal, A. Hameed and A. Suwaiyan, *Appl. Catal., A*, 2003, **243**, 165–174.

124 M. A. Gondal, A. Hameed, Z. H. Yamani and A. Arfaj, *Chem. Phys. Lett.*, 2004, **392**, 372–377.

125 J. Cheng, Z. Li, M. Haught and Y. Tang, *Chem. Commun.*, 2006, 4617–4619.

126 Y. Tang, Z. Li, W. Chen and J. Cheng, *Direct Methane Conversion to Methanol*, 2007 Spring Meeting & 3rd Global Congress on Process Safety, American Institute of Chemical Engineers, 7th Natural Gas Utilization Group, Gas Conversion and Separations Session, 92a.

127 T. Li, S. J. Wang, C. S. Yu, Y. C. Ma, K. L. Li and L. W. Lin, *Appl. Catal., A*, 2011, **398**, 150–154.

128 L. Li, G.-D. Li, C. Yan, X.-Y. Mu, X.-L. Pan, X.-X. Zou, K.-X. Wang and J.-S. Chen, *Angew. Chem.*, 2011, **123**, 8449–8453.

129 L. Yuliati, T. Hamajima, T. Hattori and H. Yoshida, *J. Phys. Chem. C*, 2008, **112**, 7223–7232.

130 H. Yoshida, N. Matsushita, Y. Kato and T. Hattori, *J. Phys. Chem. B*, 2003, **107**, 8355–8362.

131 L. Li, Y.-Y. Cai, G.-D. Li, X.-Y. Mu, K.-X. Wang and J.-S. Chen, *Angew. Chem.*, 2012, **124**, 4780–4784.

132 Y. Kato, H. Yoshida and T. Hattori, *Chem. Commun.*, 1998, 2389–2390.

133 L. Yuliati, T. Hattori and H. Yoshida, *Phys. Chem. Chem. Phys.*, 2005, **7**, 195–201.

134 C. Coperet, *Chem. Rev.*, 2009, **110**, 656–680.

135 Y. Inaki, H. Yoshida, T. Yoshida and T. Hattori, *J. Phys. Chem. B*, 2002, **106**, 9098–9106.

136 F. Sastre, V. Fornés, A. Corma and H. García, *Chem. – Eur. J.*, 2012, **18**, 1820–1825.

137 F. Sastre, V. Fornés, A. Corma and H. García, *J. Am. Chem. Soc.*, 2011, **133**, 17257–17261.

138 J. Baltrusaitis, C. de Graaf, R. Broer and E. V. Patterson, *ChemPhysChem*, 2013, **14**, 3960–3970.

139 M. Schlangen and H. Schwarz, *Catal. Lett.*, 2012, **142**, 1265–1278.

140 N. Dietl, C. van der Linde, M. Schlangen, M. K. Beyer and H. Schwarz, *Angew. Chem., Int. Ed.*, 2011, **50**, 4966–4969.

141 K. Chen, Z.-C. Wang, M. Schlangen, Y.-D. Wu, X. Zhang and H. Schwarz, *Chem. – Eur. J.*, 2011, **17**, 9619–9625.

142 J. Gao, S. Cao, Q. Tay, Y. Liu, L. Yu, K. Ye, P. C. S. Mun, Y. Li, G. Rakesh, S. C. J. Loo, Z. Chen, Y. Zhao, C. Xue and Q. Zhang, *Sci. Rep.*, 2013, **3**, 1853, DOI: 10.1038/srep01853.

143 T. A. Betley, Q. Wu, T. Van Voorhis and D. G. Nocera, *Inorg. Chem.*, 2008, **47**, 1849–1861.

144 F. Lefebvre, E. Grinenval and P. Putaj, *J. Catal.*, 2013, **2013**, 9.

145 H. Yang, T. Liu, M. Cao, H. Li, S. Gao and R. Cao, *Chem. Commun.*, 2010, **46**, 2429–2431.

146 R. Yuan, S. Fan, H. Zhou, Z. Ding, S. Lin, Z. Li, Z. Zhang, C. Xu, L. Wu, X. Wang and X. Fu, *Angew. Chem., Int. Ed.*, 2013, **52**, 1035–1039.

147 D. Shi, Y. Feng and S. Zhong, *Catal. Today*, 2004, **98**, 505–509.

148 Y. Kohno, T. Tanaka, T. Funabiki and S. Yoshida, *Phys. Chem. Chem. Phys.*, 2000, **2**, 5302–5307.

149 T. Tanaka, Y. Kohno and S. Yoshida, *Res. Chem. Intermed.*, 2000, **26**, 93–101.

150 G. Mahmodi, S. Sharifnia, F. Rahimpour and S. N. Hosseini, *Sol. Energy Mater. Sol. Cells*, 2013, **111**, 31–40.

151 M. T. Merajin, S. Sharifnia, S. N. Hosseini and N. Yazdanpour, *J. Taiwan Inst. Chem. Eng.*, 2013, **44**, 239–246.

152 N. Yazdanpour and S. Sharifnia, *Sol. Energy Mater. Sol. Cells*, 2013, **118**, 1–8.

153 K. Teramura, T. Tanaka, H. Ishikawa, Y. Kohno and T. Funabiki, *J. Phys. Chem. B*, 2003, **108**, 346–354.

154 R. R. Chianelli and B. Torres, *Photochemical processes and compositions for methane reforming using transition metal chalcogenide photocatalysts*, US20130239469A1, 2013.

155 E. Calo, A. Giannini and G. Monteleone, *Int. J. Hydrogen Energy*, 2010, **35**, 9828–9835.

156 I. M. Lorkovic, A. Yilmaz, G. A. Yilmaz, X.-P. Zhou, L. E. Laverman, S. Sun, D. J. Schaefer, M. Weiss, M. L. Noy, C. I. Cutler, J. H. Sherman, E. W. McFarland, G. D. Stucky and P. C. Ford, *Catal. Today*, 2004, **98**, 317–322.

157 A. Breed, M. F. Doherty, S. Gadewar, P. Grosso, I. M. Lorkovic, E. W. McFarland and M. J. Weiss, *Catal. Today*, 2005, **106**, 301–304.

158 M. Młotek, J. Sentek, K. Krawczyk and K. Schmidt-Szałowski, *Appl. Catal., A*, 2009, **366**, 232–241.

159 N. Yaghobi, *J. King Saud Univ., Eng. Sci.*, 2013, **25**, 1–10.

160 A. Budiman, S.-H. Song, T.-S. Chang, C.-H. Shin and M.-J. Choi, *Catal. Surv. Asia*, 2012, **16**, 183–197.

161 M. Morrill, N. Thao, P. Agrawal, C. Jones, R. Davis, H. Shou, D. Barton and D. Ferrari, *Catal. Lett.*, 2012, **142**, 875–881.

162 M. R. Morrill, N. T. Thao, H. Shou, R. J. Davis, D. G. Barton, D. Ferrari, P. K. Agrawal and C. W. Jones, *ACS Catal.*, 2013, **3**, 1665–1675.

163 K. Fang, D. Li, M. Lin, M. Xiang, W. Wei and Y. Sun, *Catal. Today*, 2009, **147**, 133–138.

164 T. F. Jaramillo, K. P. Jørgensen, J. Bonde, J. H. Nielsen, S. Horch and I. Chorkendorff, *Science*, 2007, **317**, 100–102.

This journal is © The Royal Society of Chemistry 2014

Catal. Sci. Technol., 2014, **4**, 2397–2411 | **2411**